Electronic Supplementary Information: Multiscale Modelling of the Radical-Induced Chemistry of Acetohydroxamic Acid in Aqueous Solution

Jacy K. Conrad,[a,*] Corey D. Pilgrim,[a] Simon M. Pimblott,[a] Stephen P. Mezyk,[b] and Gregory P. Horne[a,*]

[a] *Center for Radiation Chemistry Research, Idaho National Laboratory, 1955 N. Freemont Ave., Idaho Falls, 83415, USA.*

[b] *Department of Chemistry and Biochemistry, California State University Long Beach, 1250 Bellflower Boulevard, Long Beach California, 90840-9507, USA.*

*Corresponding authors. E-mail: jacy.conrad@inl.gov and gregory.horne@inl.gov

Chemicals

Acetic acid (CH_3COOH, MilliporeSigma, > 99%), acetohydroxamic acid ($CH_3CONHOH$, MilliporeSigma, 98%), ethanol (CH_3CH_2OH, MilliporeSigma, > 95%), formic acid (HCOOH, EMD Millipore Corporation, 98 – 100 %), hydroxylamine hydrochloride ($NH_2OH{\cdot}HCl$, MilliporeSigma, ≥ 99.999%, trace metals basis), hydrochloric acid (HCl, MilliporeSigma, 37%), hydroxylamine solution (HA, 50 wt.%, VWR), iron(III) chloride ($FeCl_3$, MilliporeSigma, 97%), *N*-(1-naphthyl)ethylenediamine dihydrochloride ($C_{10}H_7NHCH_2CH_2NH_2{\cdot}2HCl$, MilliporeSigma, > 98%), para-chlorobenzoic acid (*p*CBA, MilliporeSigma, 99%), perchloric acid ($HClO_4$, 70%, MilliporeSigma, ≥ 99.999%, trace metals basis), perchloric acid ($HClO_4$, Merck, 70%), potassium carbonate (K_2CO_3, MilliporeSigma, ≥ 99 %), potassium thiocyanate (KSCN, MilliporeSigma, 99%), 8-quinolinol (C_9H_7NO, MilliporeSigma, ≥ 99%), sodium nitrite ($NaNO_2$, MilliporeSigma, ≥ 99.999%, trace metals basis), sodium hydroxide (NaOH, MilliporeSigma, 50% in H_2O), sulfanilamide ($H_2NC_6H_4SO_2NH_2$, MilliporeSigma, ≥ 99%), and *tert*-butanol (*t*BuOH, VWR, 99%) were used as received without further purification. Ultra-pure water (≥ 18.2 MΩ cm) was used to prepare all solutions. Calibration gases used for gas chromatography were H_2 (1 vol% in He, Airgas), N_2O (10 vol% in He, Scotty III Analyzed Gases), and CH_4 (10 vol% in He, Airgas).

Analytical Techniques

Ultraviolet-Visible (UV-Vis) Spectroscopy

An Agilent Technologies (Santa Clara, CA, USA) Cary 6000i UV-vis spectrophotometer was used to quantify the concentrations of AHA, HA, and HNO_2 present in the solutions post-irradiation using complexation and derivatization methods. The AHA hydrolysis reaction was stopped immediately after irradiation by neutralizing the solutions with 2.0 M NaOH solution.

The concentration of AHA was determined using UV-Vis spectroscopy by monitoring the absorbance of the $Fe(CH_3CONHO)^{2+}$ complex at λ_{max} = 502 nm.[1] Up to 1 mM AHA was complexed with an excess of 5 mM $FeCl_3$ and a calibration curve of standard solutions was generated (see **Fig. S1**). A molar absorption coefficient ε = 1048.0 ± 8.9 M^{-1} cm^{-1} was calculated, consistent with that found by Andrieux *et al*.[1] This method was determined to be accurate to within ± 2 % with a limit of quantification value of 36 µM AHA.

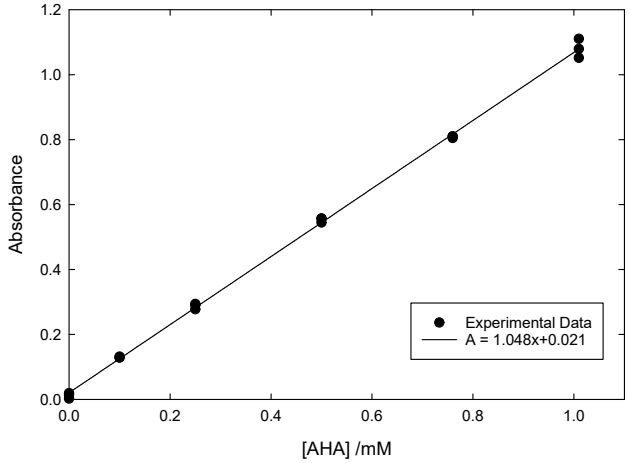

Fig. S1. Beer's law calibration curve for the UV-Vis spectrum of standard solutions of AHA in 5 mM $FeCl_3$ to form the Fe(III)-AHA complex with λ_{max} = 502 nm and fitted extinction coefficient ε_{502nm} = 1048.0 ± 8.9 L mol^{-1} cm^{-1}.

The derivatization method developed by Frear and Burrell was used to determine the concentration of HA:[2] 1 mL of 1% 8-quinolinol in ethanol and 1 mL of 1.0 M K_2CO_3 were added to 2 mL of sample and heated to 95 °C for 1 minute in closed test tubes. After being cooled for 15 minutes, the sample absorbance was measured at λ_{max} = 710 nm. The molar extinction coefficient was found to be 14213 ± 396 M^{-1} cm^{-1} (see **Fig. S2**), consistent with the reported value of ε_{705nm} = 14485 ± 364 M^{-1} cm^{-1}.[2] This method was determined to be accurate to within ± 10 %, with a limit of quantification of 17 µM HA.

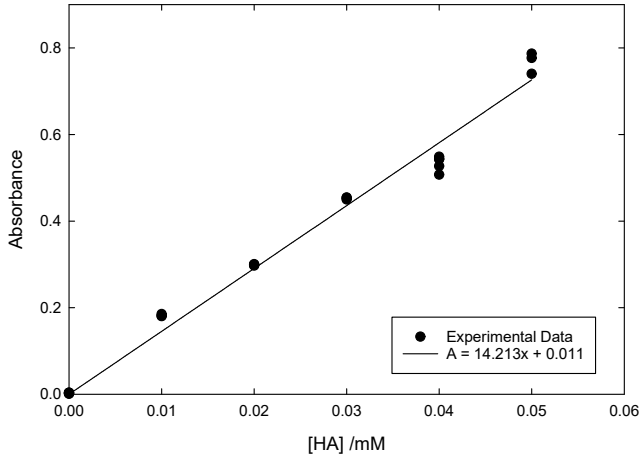

Fig. S2. Beer's law calibration curve for the UV-Vis spectrum of standard solutions of hydroxylamine hydrochloride with 8-quinolinol with λ_{max} = 710 nm and extinction coefficient ε_{710nm} = 14213 ± 396 L mol^{-1} cm^{-1}.

A modified version of the Shinn method was used to quantify the concentration of NO_2^-/HNO_2.[3] This method involved the sequential addition of 80 µL each of 58 mM sulfanilamide in 1.2 M HCl and 1.92 mM *N*-(1-naphthyl)ethylenediamine dihydrochloride to 3.84 mL of sample. The UV-visible spectrum for standard $NaNO_2$ solutions at λ_{max} = 542 nm exhibited an extinction coefficient of ε_{542nm} = 49500 ± 300 M^{-1} cm^{-1} (see **Fig. S3**), consistent with the reported literature value of ε_{543nm} = 48000 M^{-1} cm^{-1}.[3] This spectrophotometric method was determined to be accurate to within ± 4 %, and had a limit of quantification of 0.3 µM NO_2^-/HNO_2.

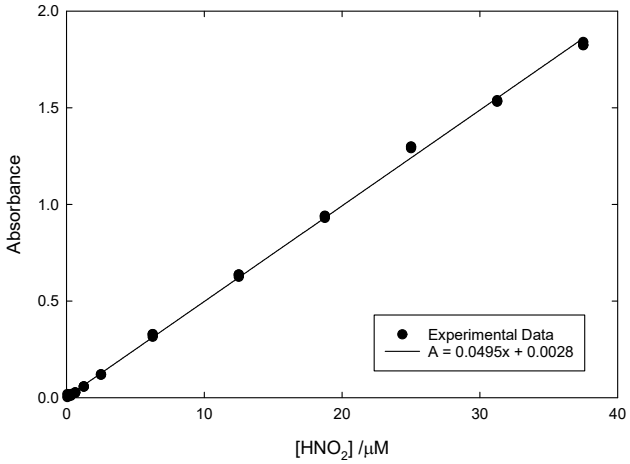

Fig. S3. Beer's law calibration curve for the UV-Vis spectrum of standard solutions of sodium nitrite treated with sulfanilamide and *N*-(1-naphthyl)ethylenediamine dihydrochloride with λ_{max} = 542 nm and extinction coefficient ε_{542nm} = 49500 ± 300 L mol^{-1} cm^{-1}.

Ion Chromatography (IC)

A Thermo Scientific (Waltham, MA, USA) Dionex ICS-5000^{+} EG ion chromatograph was used to measure the concentrations of acetate, NO_3^-/HNO_3, NO_2^-/HNO_2, and formate ions present in the AHA solutions post-irradiation, using a modified version of a standard organic acid detection method.[4] The eluent was a solution of KOH made from a EGC 500 KOH eluent generator cartridge and degassed, deionized water. The eluent was set to an initial concentration of 1 mM for 8 minutes, increased gradually to 27 mM over 12 minutes, ramped quickly to 60 mM over 0.5 minutes where it was then held for 2 minutes to flush the column, and finally decreased back to 1 mM and held for a total run time of 30 minutes per injection. The detector was a conductivity detector with eluent conductivity suppressor. The column was an IonPac AS11-HC analytical column with an AG-11-HC guard column. The column and compartment temperatures were 25 °C and the pump flow rate was 0.4 mL min^{-1}. All injections were repeated in triplicate and the results were averaged. Calibration curves for six standard solutions of 0.125 – 1.5 mM acetate, NO_3^-, NO_2^- and 0.025 – 0.5 mM formate were prepared freshly and run before every set of IC measurements. For all solutions measured, the concentrations of NO_2^-/HNO_2 and formate were below the method limit of quantification. This method was determined to be accurate to within ± 10 %.

Proton Nuclear Magnetic Resonance (^{1}H-NMR) Spectroscopy

^{1}H-NMR was used to confirm the concentrations of HA, formate, and acetate detected using UV-Vis and IC for selected doses. NMR spectra were acquired using a Bruker Avance III spectrometer at a field strength of 9.4 T (ν^1H = 400.03 MHz). An aliquot of the irradiated samples was transferred to a clean, thin-walled 5 mm NMR tube (SP Wilmad-Labglass, Vineland, NJ, USA), where d_6-DMSO (Cambridge Isotope Labs, Andover, MA, USA) inside a coaxial insert acted as both the lock solvent and chemical shift standard. The standard Bruker "zgesgp" pulse program was used, where a pulse field gradient double-echo was used to achieve water-suppression.[5] ^{1}H spectra were acquired with a hard π/2 pulse of 8.5 μsec at 29 W, a selective square-shaped π pulse of 2 msec at 1.1 mW in power, and smooth-square gradient pulses of 1 msec in duration. 16 transients were acquired after 4 dummy scans, with a sweep-width of 20 ppm and a relaxation delay of 30 sec. Data was phased and analyzed using MestReNova 12 (Mestrelab Research, Compostela, Spain).

Gas Chromatography (GC)

Radiolytically produced H_2, N_2O, and CH_4 were quantified by headspace GC measurements using a Shimadzu Co. (Kyoto, Japan) Nexus GC-2030 gas chromatograph equipped with both a barrier discharge ionization detector (BID) and a thermal conductivity detector (TCD). The H_2 and CH_4 analyses were performed using the TCD, while the N_2O analysis was done using the BID. Both detectors were at 200 °C. The injection port was set to 150 °C with a split ratio of 15. The carrier gas was helium (He) with a linear velocity of 50.0 cm s^{-1}. A Restek #19722 molecular sieve 5 Å column was used with a column oven temperature profile of 40 °C for 2 minutes, followed by a ramp to 70 °C over 2 minutes, and finally a 1-minute hold, for a total run time of 5 minutes per injection. All injections were repeated in triplicate and the results were averaged. The method was determined to be accurate to within ± 10%. Quality control checks were performed daily to confirm known concentrations relative to calibration curves measured for each of the gases.

Solutions to be irradiated and analyzed by GC were frozen in liquid nitrogen and flame-sealed inside evacuated glass ampoules prior to irradiation. Post-irradiation, a crush-tube method was employed[6-8] whereby ampoules were cracked inside a length of Nalgene 8005 braided PVC tubing that was closed on one end and fitted with a septum on the other end. The headspace of the tubing was then sampled by taking 100 µL with a Hamilton Model 1810 RN gas-tight syringe and injecting into the GC. The ampoule and tubing headspace volumes were determined by filling with water and weighing before and after cracking the ampoules. The pressure in the tubing headspace was estimated by using the ideal gas law with the calculated gas yields, the measured headspace volumes for the tubing and the ampoule, and the known pressure at which the ampoule was sealed.

Table S1. Calculated radiation track escape yields at 1 µs for the gamma radiolysis of 0.5 M AHA in water and 0.20 M $HClO_4$.

Species	**Stochastic Radiation Track Calculation Escape Yields (µmol J^{-1})**	
	0.50 M AHA in H_2O	**0.50 M AHA in 0.20 M $HClO_4$**
e_{aq}^-	< 0.001	< 0.001
H_{aq}^+	0.390	0.431
$^{\bullet}OH$	< 0.001	< 0.001
$H^{\bullet}$	0.002	0.024
H_2	0.040	0.050
OH^-	< 0.001	< 0.001
H_2O_2	0.055	0.057
$O(^3P)$	0.005	0.004
O_2	< 0.001	< 0.001
$HO_2^{\bullet}$	0.001	0.001
O^-	< 0.001	< 0.001
$O_2^{\bullet-}$	< 0.001	< 0.001
HO_2^-	< 0.001	< 0.001
H_2O	0.340	0.627
$CH_3C^{\bullet}(OH)NHOH$	0.399	0.370
$CH_3CONHO^{\bullet}$	0.371	0.368

Table S2. The reaction set used in addition to an existing water radiolysis model[9] to simulate the radiolysis and hydrolysis of acetohydroxamic acid and its degradation products.

#	Chemical Reaction	Rate Coefficient[a] at 25 °C	Source
1	$CH_3CONHOH + H_3O^+ \rightarrow CH_3COOH + NH_3OH^+$	3.92×10^{-5}	10
2	$CH_3CONHOH + {}^{\bullet}CH_3 \rightarrow CH_4 + CH_3CONHO^{\bullet}$	4×10^{3}	Proposed rate, based on similar reactions in ref 11
3	$CH_3CONHOH + {}^{\bullet}CONHOH \rightarrow HCONHOH + CH_3CONHO^{\bullet}$	1×10^{8}	Proposed rate, based on similar reactions in ref 11
4	$HCONHOH + H_2O \rightarrow HCOOH + NH_2OH$	1×10^{-4}	Proposed rate, based on similar reactions in ref 12
5	$CH_3CONHOH + {}^{\bullet}OH \rightarrow H_2O + CH_3CONHO^{\bullet}$	4.75×10^{8}	This work
6	$CH_3CONHOH + e_{aq}^- \rightarrow CH_3C^{\bullet}(O^-)NHOH$	6.02×10^{8}	This work
7	$CH_3CONHOH + H^{\bullet} \rightarrow CH_3C^{\bullet}(OH)NHOH$	5.43×10^{6}	This work
8	$CH_3CONHOH + {}^{\bullet}CH_2COOH \rightarrow CH_3COOH + CH_3CONHO^{\bullet}$	1×10^{8}	Proposed rate based on similar reactions in ref 11
9	$2CH_3CONHO^{\bullet} \rightarrow CH_3CONHOH + CH_3CON{=}O$	1.51×10^{9}	This work
10	$CH_3CON{=}O + H_2O \rightarrow CH_3COOH + HNO$	1	Proposed rate, reaction from refs 13, 14
11	$CH_3COOH + e_{aq}^- \rightarrow CH_3COO^- + H^{\bullet}$	2.2×10^{8}	15
12	$CH_3COOH + {}^{\bullet}OH \rightarrow {}^{\bullet}CH_2COOH + H_2O$	1.5×10^{7}	16
13	$CH_3COOH + H^{\bullet} \rightarrow {}^{\bullet}CH_2COOH + H_2$	8.4×10^{4}	17
14	$CH_3COO^- + e_{aq}^- \rightarrow$ products	1.1×10^{6}	18
15	$CH_3COO^- + {}^{\bullet}OH \rightarrow {}^{\bullet}CH_2COO^- + H_2O$	9×10^{7}	19
16	$CH_3COO^- + H^{\bullet} \rightarrow {}^{\bullet}CH_2COO^- + H_2$	4.2×10^{5}	20
17	$NH_2OH + e_{aq}^- \rightarrow OH^- + {}^{\bullet}NH_2$	9.2×10^{8}	21
18	$NH_2OH + {}^{\bullet}OH \rightarrow H_2O + {}^{\bullet}NH_2O$	9.5×10^{9}	21
19	$NH_3OH^+ + e_{aq}^- \rightarrow {}^{\bullet}OH + NH_3$	2.55×10^{9}	This work
20	$NH_3OH^+ + {}^{\bullet}OH \rightarrow H_2O + {}^{\bullet}NH_3O^+$	1.59×10^{9}	This work
21	$NH_3OH^+ + H^{\bullet} \rightarrow H_2 + {}^{\bullet}NH_3O^+$	4.01×10^{5}	This work
22	$NH_3OH^+ + H_2O_2 \rightarrow {}^{\bullet}NH_3O^+ + {}^{\bullet}OH + H_2O$	2.2×10^{-4}	22
23	${}^{\bullet}NH_2O + {}^{\bullet}NH_2O \rightarrow N_2 + 2H_2O$	4.5×10^{8}	21
24	${}^{\bullet}NH_2O + O_2 \rightarrow HNO + {}^{\bullet}HO_2$	1×10^{4}	Proposed rate, reaction from ref 23
25	${}^{\bullet}NH_2O + H_2O_2 \rightarrow HNO + {}^{\bullet}OH + H_2O$	150	Proposed rate, reaction from refs 21, 22
26	${}^{\bullet}NH_3O^+ + H_2O_2 \rightarrow HNO + {}^{\bullet}OH + H_2O + H^+$	10	Proposed rate, reaction from refs 21, 22
27	$HNO + HNO \rightarrow N_2O + H_2O$	8×10^{6}	24
28	$CH_3C^{\bullet}(OH)NHOH \rightarrow CH_3CHO + NH_2O^{\bullet}$	1×10^{7}	Proposed rate based on reactions in refs 25, 26
29	$N_2O + e_{aq}^- \rightarrow O^- + N_2$	9.6×10^{9}	27
30	$N_2O + H^{\bullet} \rightarrow N_2 + {}^{\bullet}OH$	9×10^{4}	28
31	$CH_3CHO + e_{aq}^- \rightarrow$ products	4.4×10^{9}	29
32	$CH_3CHO + H^{\bullet} \rightarrow {}^{\bullet}CH_3CO + H_2$	3.1×10^{7}	17

33	$CH_3CHO + {}^{\bullet}OH \rightarrow H_2O + {}^{\bullet}CH_3CO$	3.6×10^9	30
34	${}^{\bullet}CH_3CO + {}^{\bullet}CH_3CO + H_2O \rightarrow CH_3COOH + CH_3CHO$	7.5×10^7	31
35	$CH_3CHO + CH_3CHO + H_2O_2 \rightarrow CH_3COOH + CH_3COOH$	0.66	32

[a] units: $M^{-1}s^{-1}$ for second order, s^{-1} for first order.

Table S3. The acid-base equilibria included in the model in addition to those from existing water and nitrate models.

#	Chemical Reaction	pK_a at 25 °C[a]
1	$CH_3CONHOH + H_2O \rightleftharpoons CH_3CONHO^- + H_3O^+$	8.7
2	${}^{\bullet}CH_3CONHO + H_2O \rightleftharpoons {}^{\bullet}CH_3CONO^- + H_3O^+$	9.1
3	$CH_3COOH + H_2O \rightleftharpoons CH_3COO^- + H_3O^+$	4.75
4	$NH_3OH^+ + H_2O \rightleftharpoons NH_2OH + H_3O^+$	6.17
5	${}^{\bullet}NH_3O^+ + H_2O \rightleftharpoons {}^{\bullet}NH_2O + H_3O^+$	4.2

[a] For the 1 mol L^{-1} standard reference state

Summary of Rate Coefficients Determined in this Work

$CH_3CONHOH + e_{aq}^-$

The rate coefficient determined for the reaction of the hydrated electron with acetohydroxamic acid was $k(CH_3CONHOH + e_{aq}^-) = (6.02 \pm 0.86) \times 10^8\ M^{-1}s^{-1}$, which is within the experimental uncertainty of value of $(6.4 \pm 0.2) \times 10^8\ M^{-1}s^{-1}$ reported by Samuni and Goldstein[33].

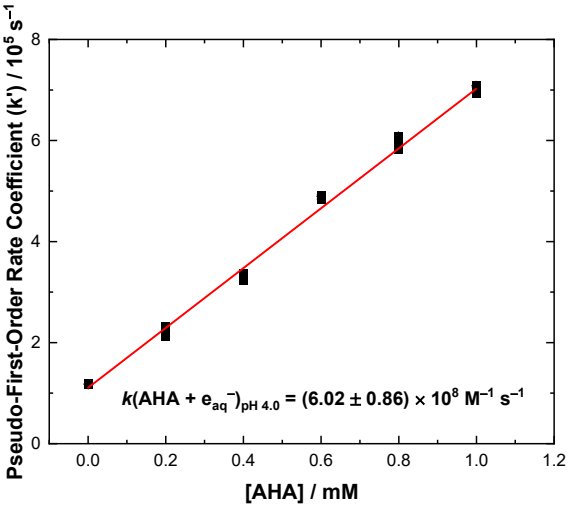

Fig. S4. Determination of the second order rate coefficient for the reaction of the hydrated electron with acetohydroxamic acid at pH 4.0 using pseudo-first-order rate coefficients found from exponential growth fits to raw kinetic data.

$CH_3CONHOH + {}^{\bullet}OH$

The rate constant for the reaction between the hydroxyl radical and acetohydroxamic acid was determined using the thiocyanate anion as a competitor for the hydroxyl radical using $k(SCN^- + {}^{\bullet}OH) = 1.1 \times 10^{10}\ M^{-1}s^{-1}$.[34] The change in the dose-corrected absorption of a 103.85 µM solution of KSCN with the

addition of different concentrations of AHA was fitted with a linear function to determine the ratio of the rate coefficients for their reactions with •OH. This yielded a second order rate constant of $k(CH_3CONHOH + {}^{\bullet}OH) = (4.75 \pm 0.76) \times 10^8\ M^{-1}s^{-1}$. Samuni and Goldstein[33] found a value of $k(CH_3CONHOH + {}^{\bullet}OH) = (2.7 \pm 0.2) \times 10^8\ M^{-1}s^{-1}$, using competition kinetics with $ABTS^{2-}$.

$CH_3CONHO^- + {}^{\bullet}OH$

The rate constant for the reaction between the hydroxyl radical and deprotonated acetohydroxamic acid was determined using the thiocyanate anion as a competitor for •OH. The ratio of the rate coefficients for SCN^- and CH_3CONHO^- reacting with •OH was fitted, yielding an "effective rate coefficient" of $k_{eff} = (3.47 \pm 0.10) \times 10^9\ M^{-1}s^{-1}$. At pH 9.8, 10.7 % of the AHA remains as protonated $CH_3CONHOH$, and therefore, to isolate the rate constant for just CH_3CONHO^-, the following relationship is used:

$$k_{eff}([CH_3CONHOH] + [CH_3CONHO^-]) = k_5[CH_3CONHOH] + k_9[CH_3CONHO^-] \quad \textbf{(1)}$$

The resulting rate coefficient is $k(CH_3CONHO^- + {}^{\bullet}OH) = (3.86 \pm 0.11) \times 10^9\ M^{-1}s^{-1}$, which is within uncertainty of the value $(4.0 \pm 0.1) \times 10^9\ M^{-1}s^{-1}$ reported by Samuni and Goldstein[33] at pH 11 from competition kinetics with $ABTS^{2-}$. As expected from the electrophilic nature of •OH, the reaction with unprotonated AHA is significantly faster than with the protonated species.

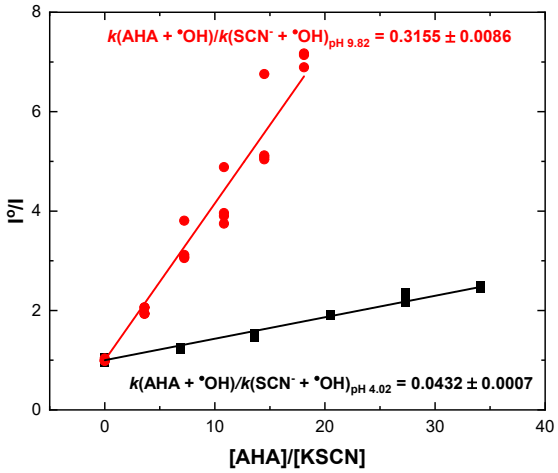

Fig. S5. Determination of the ratio of the rate coefficients for the reactions of the hydroxyl radical with acetohydroxamic acid and with the thiocyanate anion from linear fits of the dose-corrected absorption ratio against the concentration ratio for 103.85 µM KSCN at pH 9.8 (**red**) and pH 4.0 (**black**).

$CH_3CONHOH + {}^{\bullet}H$

The second order rate constant for the reaction between the hydrogen atom and acetohydroxamic acid was found to be $k(CH_3CONHOH + {}^{\bullet}H) = (5.43 \pm 0.56) \times 10^6\ M^{-1}s^{-1}$. Previous authors[33] were able to determine that the rate of this reaction was $< 1 \times 10^7\ M^{-1}s^{-1}$ by using competition kinetics with phenol, consistent with our result.

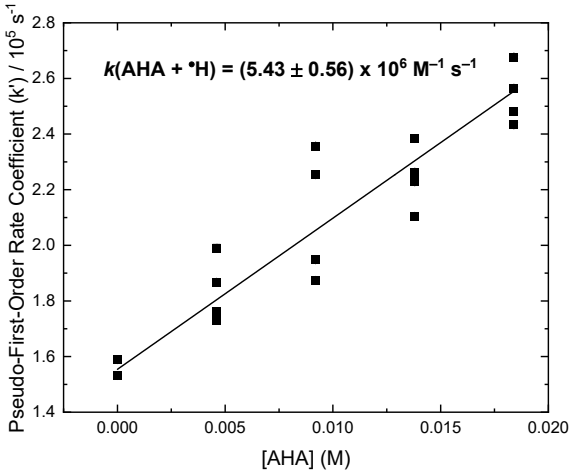

Fig. S6. Determination of the second order rate coefficient for the reaction of the hydrogen atom with acetohydroxamic acid using pseudo-first-order rate coefficients found from exponential growth fits to raw kinetic data of competitor p-chlorobenzoic acid adduct.

$CH_3CONHO^{\bullet}$ + $CH_3CONHO^{\bullet}$

The rate coefficient $k(CH_3CONHO^{\bullet} + CH_3CONHO^{\bullet}) = (1.51 \pm 0.02) \times 10^9\ M^{-1}s^{-1}$ was found for the bimolecular combination of the transient AHA nitroxide radical by fitting the radical decay at 260 nm. This rate coefficient was independent of AHA concentration and dose. Previous authors[33] found a significantly slower rate constant of $2k(CH_3CONHO^{\bullet} + CH_3CONHO^{\bullet}) = (8.7 \pm 1.3) \times 10^7\ M^{-1}s^{-1}$, which is inconsistent with the expected rates for this type of reaction. These same authors[33] found rates for the combination of the deprotonated radicals: $2k(CH_3CONO^{\bullet-} + CH_3CONO^{\bullet-}) = (5.6 \pm 0.4) \times 10^7\ M^{-1}s^{-1}$, and a combination of the protonated and deprotonated radical: $2k(CH_3CONO^{\bullet-} + CH_3CONHO^{\bullet}) = (8.7 \pm 1.3) \times 10^8\ M^{-1}s^{-1}$ that are more consistent with the protonated radical recombination rate measured in this work.

$NH_3OH^+ + e_{aq}^-$

The reaction between protonated hydroxylamine and the hydrated electron, although originally predicted to yield the amino radical, $^{\bullet}NH_3^+$, and hydroxide[21], has since been proven[35] to take the form:

$$NH_3OH^+ + e_{aq}^- \rightarrow NH_3 + {}^{\bullet}OH \qquad \text{(R19)}$$

The rate coefficient for this reaction was determined to be $k(NH_3OH^+ + e_{aq}^-) = (2.55 \pm 0.10) \times 10^9\ M^{-1}s^{-1}$ at pH 4.0. This rate constant is lower than the value of $(1.2 \pm 0.1) \times 10^{10}\ M^{-1}s^{-1}$ reported in the original study by Simic and Hayon[21].

$NH_3OH^+ + {}^{\bullet}H$

The rate constant for the reaction between the hydrogen atom and hydroxylamine was determined as $k(NH_3OH^+ + {}^{\bullet}H) = (4.01 \pm 0.43) \times 10^5\ M^{-1}s^{-1}$. This is the first time that this rate constant has been reported.

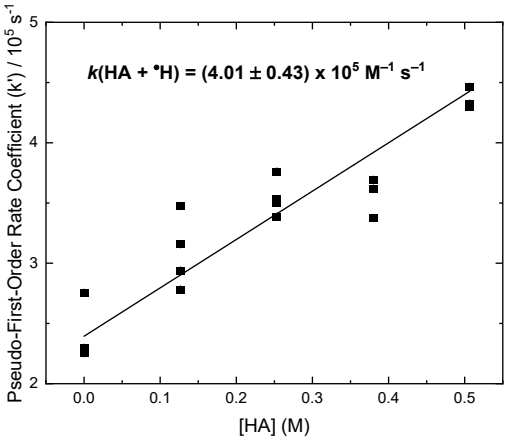

Fig. S7. Determination of the second order rate coefficient for the reaction of the hydrogen atom with hydroxylamine in 3 M $HClO_4$ using pseudo-first-order rate coefficients found from exponential growth fits to raw kinetic data.

NH_3OH^+ + •OH

The second order rate constant for the reaction between hydroxylamine and the hydroxyl radical was determined using competition kinetics with a 100.2 µM solution of KSCN at pH 3.98. The value found in this work, $k(NH_3OH^+ + {}^\bullet OH) = (1.59 \pm 0.06) \times 10^9\ M^{-1}s^{-1}$, is consistent with the results from Simic and Hayon[21] obtained using the same method. Although they reported a value of $(5 \pm 0.5) \times 10^8\ M^{-1}s^{-1}$, these authors suggested that the actual rate coefficient may be somewhat higher than the one that they observed.

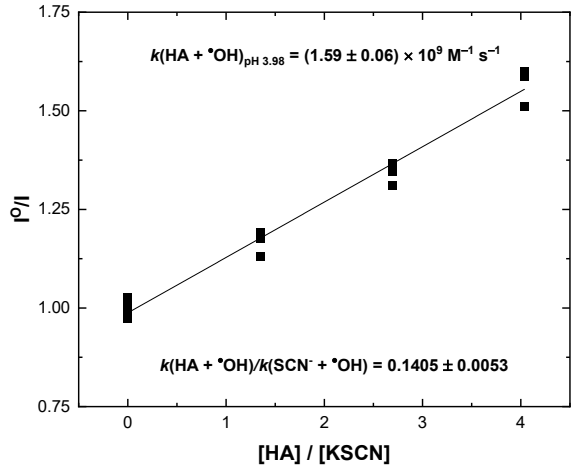

Fig. S8. The second order rate coefficient for the reaction of the hydroxyl radical with hydroxylamine determined relative to the thiocyanate anion by plotting the dose-corrected absorption ratio against the concentration ratio for 100.2 µM KSCN at pH 3.55.

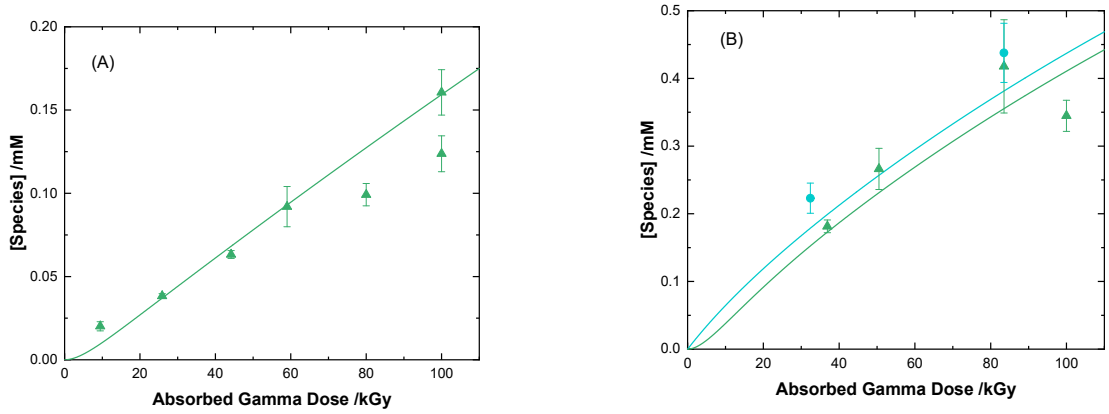

Fig. S9. Concentrations of CH_4 (▲) and HCOOH (ᔓ) as a function of absorbed gamma dose in **(A)** water and **(B)** 0.20 M $HClO_4$ at 51 Gy min^{-1} at 36 °C as determined from gas chromatography and ^{1}H-NMR. Curves are predicted values from multiscale modeling calculations.

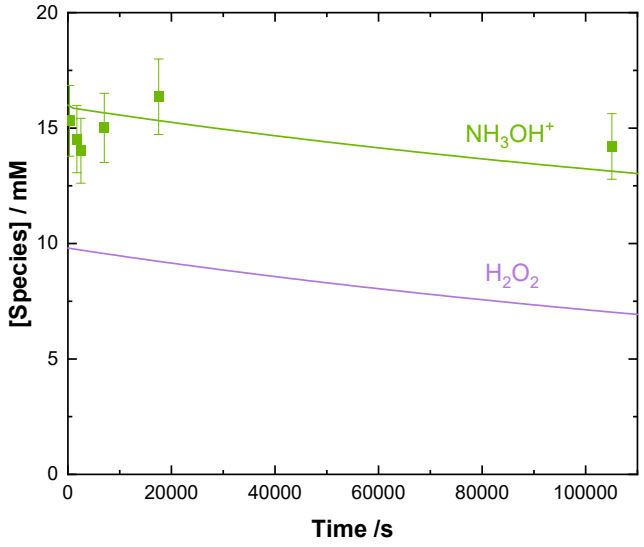

Fig. S10. The experimental concentration of hydroxylamine as a function of time for an aqueous solution of 16 mM HA and 9.8 mM H_2O_2. Model predictions for both species are shown by the solid curves.

REFERENCES

1. F. P. L. Andrieux, C. Boxall and R. J. Taylor, *J. Solut. Chem.*, 2007, **36**, 1201-1217.

2. D. S. Frear and R. C. Burrell, *Anal. Chem.*, 1955, **27**, 1664-1665.

3. K. Bendschneider and R. J. Robinson, *A new spectrophotometric method for the determination of nitrite in sea water*, Report 8, University of Washington, Oceanographic Laboratories, 1952.

4. L. Chen, B. De Borba and J. Rohrer, *Determination of Organic Acids in Fruit Juices and Wines by High-Pressure IC*. Thermo Fisher Scientific Application Note. 2013.

5. T. L. Hwang and A. J. Shaka, *J. Magn. Reson., Ser. A*, 1995, **112**, 275-279.

6. J. A. Laverne and R. H. Schuler, *J. Phys. Chem.*, 1984, **88**, 1200-1205.

7. J. A. LaVerne and P. L. Huestis, *J. Phys. Chem. C*, 2019, **123**, 21005-21010.

8. E. H. Parker-Quaife, C. Verst, C. R. Heathman, P. R. Zalupski and G. P. Horne, *Radiat. Phys. Chem.*, 2020, **177**.

9. A. J. Elliot and D. M. Bartels, *The Reaction Set, Rate Constants and G-Values for the Simulation of the Radiolysis of Light Water Over the Range 20° to 350°C Based on Information Available in 2008*, Report 153-127160-450-001, AECL Nuclear Platform Research and Development, 2009.

10. F. P. L. Andrieux, C. Boxall, H. M. Steele and R. J. Taylor, *J. Solut. Chem.*, 2014, **43**, 608-622.

11. P. Neta, J. Grodkowski and A. B. Ross, *J. Phys. Chem. Ref. Data*, 1996, **25**, 709-1043.

12. R. W. Taft, *J. Am. Chem. Soc.*, 1952, **74**, 2729-2732.

13. E. Maimon, A. Lerner, A. Samuni and S. Goldstein, *J. Phys. Chem. A*, 2018, **122**, 7006-7013.

14. A. S. Evans, A. D. Cohen, Z. A. Gurard-Levin, N. Kebede, T. C. Celius, A. P. Miceli and J. P. Toscano, *Can. J. Chem.*, 2011, **89**, 130-138.

15. D. Razem and W. H. Hamill, *J. Phys. Chem.*, 1977, **81**, 1625-1631.

16. J. K. Thomas, *Trans. Faraday Soc.*, 1965, **61**, 702-707.

17. P. Neta, R. W. Fessenden and R. H. Schuler, *J. Phys. Chem.*, 1971, **75**, 1654-1666.

18. G. Kohler, S. Solar, N. Getoff, A. R. Holzwarth and K. Schaffner, *J. Photochem.*, 1985, **28**, 383-391.

19. R. L. Willson, C. L. Greenstock, G. E. Adams, R. Wageman and L. M. Dorfman, *Int. J. Radiat. Phys. Chem.*, 1971, **3**, 211-220.

20. P. Neta and R. H. Schuler, *J. Phys. Chem.*, 1972, **76**, 2673-2679.

21. M. Simic and E. Hayon, *J. Am. Chem. Soc.*, 1971, **93**, 5982-5986.

22. L. W. Chen, X. C. Li, J. Zhang, J. Y. Fang, Y. M. Huang, P. Wang and J. Ma, *Environ. Sci. Technol.*, 2015, **49**, 10373-10379.

23. N. K. V. Leitner, P. Berger, G. Dutois and B. Legube, *J. Photochem. Photobiol. A-Chem.*, 1999, **129**, 105-110.

24. V. Shafirovich and S. V. Lymar, *Proceedings of the National Academy of Sciences of the United States of America*, 2002, **99**, 7340-7345.

25. M. Murakami and N. Ishida, *Chemistry Letters*, 2017, **46**, 1692-1700.

26. M. Bietti, O. Lanzalunga and M. Salamone, *J. Org. Chem.*, 2005, **70**, 1417-1422.

27. A. J. Elliot, *Radiat. Phys. Chem.*, 1989, **34**, 753-758.

28. L. Kazmierczak, D. Swiatla-Wojcik and M. Wolszczak, *RSC Adv.*, 2017, **7**, 8800-8807.

29. G. Duplatre and C. D. Jonah, *Radiat. Phys. Chem.*, 1984, **24**, 557-565.

30. M. N. Schuchmann and C. von Sonntag, *J. Am. Chem. Soc.*, 1988, **110**, 5698-5701.

31. D. Santiard, D. Sabourault, C. Ribière, R. Nordmann, C. Houée-Levin and C. Ferradini, *J. Chim. Phys. Phys.-Chim. Biol.*, 1991, **88**, 967-976.

32. C. S. Satterfield and L. C. Case, *Ind. Eng. Chem.*, 1954, 998 - 1001.

33. A. Samuni and S. Goldstein, *J. Phys. Chem. A*, 2011, **115**, 3022-3028.

34. G. V. Buxton, C. L. Greenstock, W. P. Helman and A. B. Ross, *J. Phys. Chem. Ref. Data*, 1988, **17**, 513-886.

35. P. Neta, P. Maruthamuthu, P. M. Carton and R. W. Fessenden, *J. Phys. Chem.*, 1978, **82**, 1875 - 1878.